Micro and Nano Systems Letters

LETTER Open Access

In-vivo recording of sensory signals from peripheral nerves using flexible 3D neural electrodes

Byungwook Park[1], Jae-Won Jang[1] and Sohee Kim[1*]

Abstract

To overcome the limitations of muscle-based prostheses, studies on nerve-based prostheses for sensory feedback have recently been reported. To develop such prostheses, intrafascicular electrodes, a type of peripheral nerve interface, are essentially used to connect the nervous system and external systems. Through these electrodes, sensory feedback to induce sensations in patients is possible. To evoke natural sensations, precise recordings of nerve signals should precede sensory feedback, in order to identify patterns of sensory signals in the nerve and to mimic these patterns in stimulating the nerve. For this purpose, we previously developed a PDMS-based flexible penetrating microelectrode array (FPMA). In the current study, we verified the ability of the FPMA to record sensory nerve signals. The FPMA implanted in the rabbit sciatic nerve was able to record spontaneous neural signals, and the recorded signals were separated into action potential units. In addition, sensory nerve signals synchronized with ankle movement were successfully recorded, demonstrating that the FPMA is a useful peripheral neural interface capable of recording high-resolution sensory signals.

Keywords Flexible penetrating microelectrode array (FPMA), Neural interface, Peripheral neural interface, Peripheral neural recording

Introduction

To restore the amputee's motor ability, several muscle-based prostheses have been developed [1–3]. However, these prostheses have limitations in that control of fine movement is difficult and natural sensory feedback is impossible [2, 4, 5]. To overcome these limitations, nerve-based prostheses that can directly interact with nerves have been emerging [6, 7]. Peripheral neural interfaces are widely used in such nerve-based prosthetics studies [7–9]. Among various types of peripheral neural interfaces, the majority of nerve-based prosthetic studies for sensory feedback have used intrafasicular electrodes due to their high resolution in recording and high selectivity in stimulation [7, 8, 10].

However, the studies on sensory feedback rely on simple non-specific nerve stimulation strategies. As the result, the evoked sensation is not quite natural, and there is a big difference from the natural sensations experienced in real life [8, 10]. It is because simple nerve stimulation does not properly mimic the complexity of encoded sensory signals in the nerve [11]. To generate natural sensations, it is necessary to identify the specific sensory signals passing through the nerve and at what frequency they are encoded. Afterward, the peripheral neural interface must stimulate the nerve according to the specific patterns of sensory signals at the exact

*Correspondence:
Sohee Kim
soheekim@dgist.ac.kr
[1]Department of Robotics and Mechatronics Engineering, Daegu Gyeongbuk Institute of Science and Technology (DGIST), Daegu, South Korea

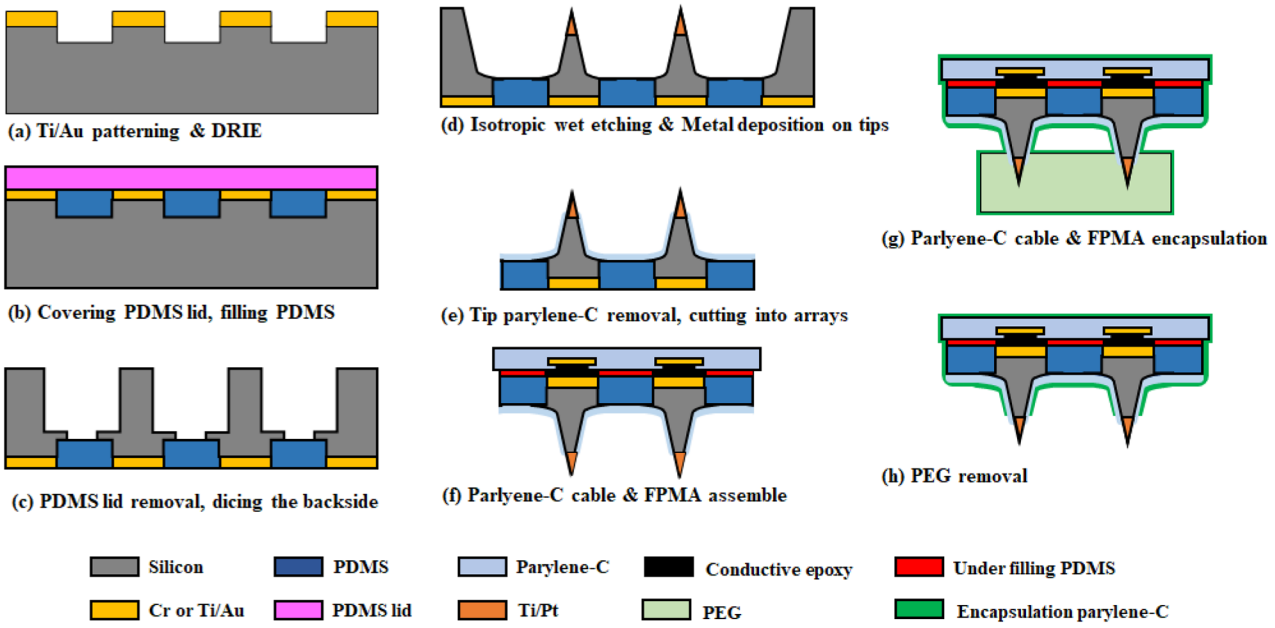

Fig. 1 Schematic illustration of the FPMA fabrication procedures

location where the sensory signal passes. Therefore, to induce natural sensations, the peripheral nerve interface needs to possess the ability to record sensory-evoked neural signals accurately [11]. However, most of the currently used intrafascicular electrodes focus on stimulation, so their ability to record peripheral nerve signals is not sufficiently validated [7, 10, 12].

Among several intrafascicular electrodes, the Utah slanted electrode array (USEA) is the only electrodes with proven neural stimulation and neural recording capabilities [8, 13]. However, the USEA is rigid and inflexible as it is fabricated based on silicon. Therefore, the USEA has the limitations when applied to peripheral nerves with large curvature. In addition, due to its stiffness, the mismatch in physical properties with the peripheral nervous tissues is severe, resulting in strong immune responses [14, 15]. For this reason, it is required to develop a peripheral nerve interface that is flexible to fit the curvature of the peripheral nerves and has soft properties to reduce the immune responses.

We previously developed a polydimethylsiloxane (PDMS)-based flexible penetrating microelectrode array (FPMA) through MESM-based technology [16]. Because the FPMA is based on flexible PDMS rather than silicon, it is flexible to fit the shape of the nerve and lowers the immune response [17]. Here, we investigate the ability of the FPMA to record peripheral neural signals in response to various stimuli.

Methods

Fabrication of peripheral nerve signal recording system

The peripheral neural signal recording system was fabricated by integrating the FPMA and an interconnection cable.

The FPMA is a needle-shaped electrode array with PDMS-based flexible substrate, as previously presented [16, 17]. Each of the electrodes is used as a probe to sense the changes in electrical potential around it, so highly doped silicon was used as conductor material. At first, Ti/Au with thicknesses of 50 nm/200 nm, respectively, were sputtered and patterned (SRN-110, Sorona Inc., Anseong, Korea). The silicon wafer was etched about 200 μm deep using deep reactive ion etching in an array pattern (LPX PEGASUS, SPTS Technologies Ltd, Newport, UK), except for the sputtered part (Fig. 1a). We covered sputtered Au pads with a PDMS lid to prevent further contamination during the next fabrication steps. To build a flexible base of FPMA, liquid PDMS was filled in the etched trenches and cured at 60 ℃ for 2 h (Fig. 1b). After removing the PDMS lid, a square columnar array was fabricated through a dicing process (Fig. 1c). The needle-like shape of electrodes was created by wet etching using HNA solution. The tips of electrodes were sputtered with Ti/Pt in thicknesses of 50 nm/200nm to reduce the impedance of the active electrode sites (Fig. 1d). Except for the Au-sputtered pads and the tips of the electrodes, parylene-C with a thickness of 3 μm was deposited by a low-pressure chemical vapor deposition process using a parylene coating system for insulation (NRPC-500, Nuritech, Goyang, Korea) (Fig. 1e).

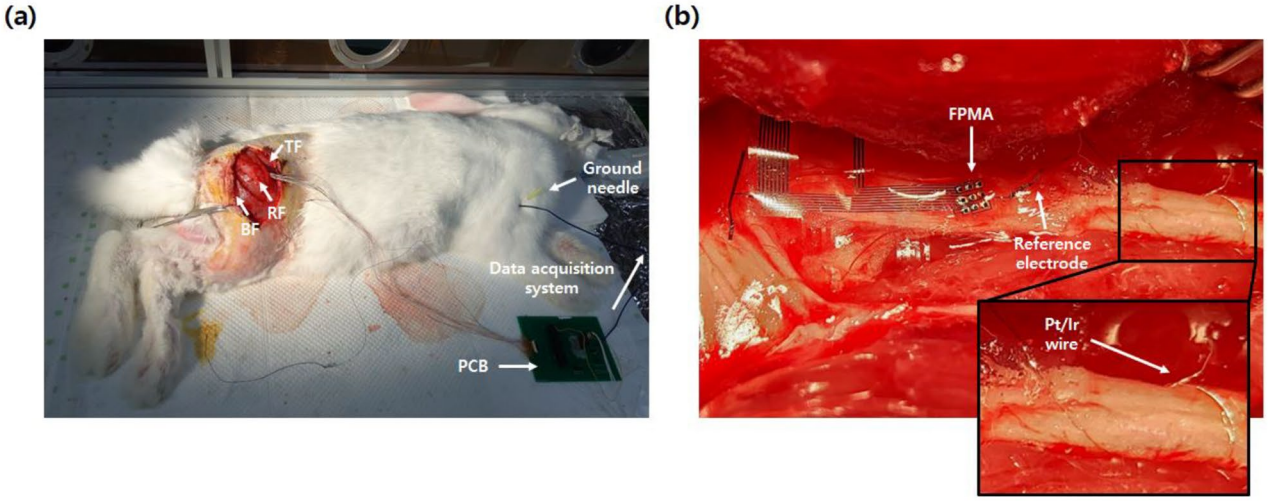

Fig. 2 Experimental setup for acute recording from the sciatic nerve in a rabbit. (a) An FPMA was inserted between BF and RF muscles and the cable came out through the space between RF and TF muscles. The wires were connected to the data acquisition system through a PCB. A ground needle was inserted into the skin of the forelimb (BF: biceps femoris muscle. RF: rectus femoris muscle. TF: tensor fasciae latae muscle). (b) A magnified view of the FPMA implanted on the sciatic nerve. A flat electrode based on the parylene-C cable and a Pt/Ir wire were used as reference electrodes

Next, we fabricated a custom interconnection cable for use in *in-vivo* experiments. The interconnection cable was composed of a parylene-C based cable, custom-designed flexible printed circuit boards (FPCBs), and ultra-thin wires. The parylene-C based cable was fabricated by stacking parylene-C and metal layers. The first layer of parylene-C was deposited about 3 μm on a titanium sputtered silicon wafer. And we sputtered Ti/Au with thicknesses of 50 nm/200nm, respectively, and patterned for conductive lines. The second layer of parylene-C was coated around 3 μm to insulate the conductive lines. The parylene-C was etched using reactive ion etching (RIE) to open connection pads and outline the cable. The parylene-C based cable was obtained by immersing the wafer in Ti etchant (hydrofluoric acid solution). The parylene-C based cable was connected to the FPCBs that were used as the adapter boards, using conductive epoxy (Duralco 125, Cotronics, New York, NY, US), and wires were soldered to connect the FPCBs. To prevent toxic reactions in *in-vivo*, we encapsulated the soldered portion entirely using PDMS.

The fabricated electrodes were cut into the size of the array, and integrated with the parylene-C-based cable using conductive epoxy. PDMS filled the gap formed between the cable and the FPMA, for mechanical and electrical stability, and cured at 60 ℃ for 2 h (Fig. 1f). The integrated neural interface was coated with 2 μm thick Parylene-C, which has excellent biocompatibility, for implantation in *in-vivo*. At this step, the tips of the electrodes were protected using polyethylene glycol (PEG) (Fig. 1 g). By removing PEG and cleaning the active electrode sites, we could obtain the completed peripheral neural interface device (Fig. 1 h).

Surgical procedures

All surgical procedures for animal experiments were approved by the Institutional Animal Care and Use Committee (IACUC) of DGIST (Approval No. DGIST-IACUC-22022502-0003). The FPMA was implanted onto the sciatic nerve of a New Zealand White (NZW) rabbit weighing more than 4 kg and over 1 year old, which was however selected by weight rather than age. To prevent infection, the FPMA and the recording equipment were sterilized with hydrogen peroxide before surgery. The rabbit was first anesthetized using ketamine/xylazine, and then tracheal intubation was performed during anesthesia. Anesthesia was maintained using 2.5% isoflurane. The fur on the legs was shaved before surgery. Biceps femoris (BF) and rectus femoris (RF) muscles were opened to expose the sciatic nerve. To stably implant the FPMA into the sciatic nerve, RF and tensor fasciae latae muscles (TF) were additionally spread apart. The FPMA was then placed near the nerve through the BF and RF muscles. The wires attached to the FPMA came out through the space between the RF and TF muscles and were connected to the printed circuit board (PCB) (Fig. 2a). The FPMA was carefully placed 2-3 cm proximal from the tibial and peroneal branches and inserted into the sciatic nerve using an inserter (NeuroPort Electrode Inserter System, Blackrock Neurotech, Salt Lake City, UT, USA). A Pt/Ir wire wound on the distal part of the electrodes and a flat electrode attached to the parylene-C cable were used as reference electrodes, as shown in Fig. 2b. A ground electrode, made of a syringe needle, was inserted into the skin of the forelimb as shown in Fig. 2a.

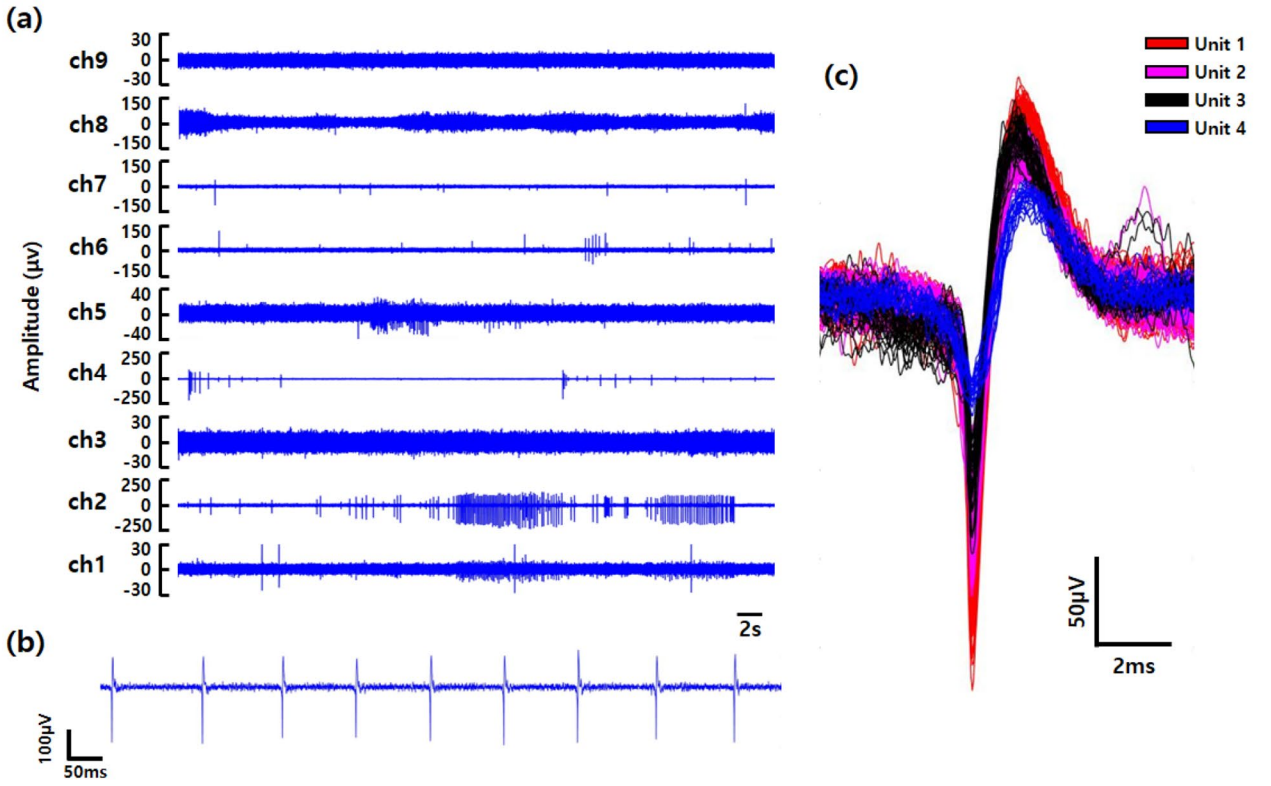

Fig. 3 Spontaneous neural signals recorded by an FPMA implanted in the sciatic nerve. (a) Spontaneous action potentials were recorded by 6 out of 9 channels. On channel 8, compound action potentials were recorded. (b) Magnified view of the neural signal recorded on channel 2. (c) Single spike units were detected from channel 2. Four spike units were separated

Acute *in-vivo* recording and signal processing

After surgery, the rabbit was placed in a custom-made faraday cage to minimize electromagnetic interferences. Neural signals were recorded using a data acquisition system (Cereplex™, Blackrock Neurotech, Salt Lake City, UT, USA), at a 30 kHz sampling rate. In addition, noises were removed using a 250-5000 Hz bandpass filter provided by the data acquisition system. To minimize movement artifacts during recording, we grabbed the rabbit's paw and waited until the signals were stabilized. Once stabilized, the rabbit's ankle was moved slowly, taking care not to move the entire leg. All of these processes were recorded by a camera, and neural signals and ankle movements were synchronized through recorded videos.

The recorded neural signals were analyzed with commercial software Matlab (Mathworks, Natick, MA, USA) and SPIKE 2 (CED, Cambridge, UK). The signal-to-noise ratio (SNR) was calculated using the following equation [17, 18].

$$\mathrm{SNR} = \frac{average of action potential amplitude}{2 \times standard deviation of noise}$$

Results

Spontaneous neural spike recording

Spontaneous neural signals were detected by 7 out of 9 channels of the FPMA. Unit action potentials (APs), so called 'spikes', were recorded by 6 out of 7 channels, while one channel (ch. 8) recorded only compound action potentials. Except for adjacent channels 1 and 2, the recorded neural signals had all different waveforms depending on channels (Fig. 3a). Through this observation, it was confirmed that the signal recorded by each channel of the FPMA was a signal generated from the nervous tissue around the electrode, not from external noises such as muscle signals or respiration. We could also confirm that the flexible FPMA was stably implanted into the nerve according to the curve of the sciatic nerve and that each channel was located adjacent to different axons. It showed that the FPMA was an efficient tool capable of recording multiple axons within the peripheral nerve.

In particular, burst-type multi-unit neural signals were detected in channels 1, 2, and 5 (Fig. 3a). These recorded multi-unit spontaneous signals exhibited a spike period of about 0.3 to 0.4 s in one burst (Fig. 3b). It has been reported that such neural signals are generated by the activation of c-nociceptive axon following peripheral

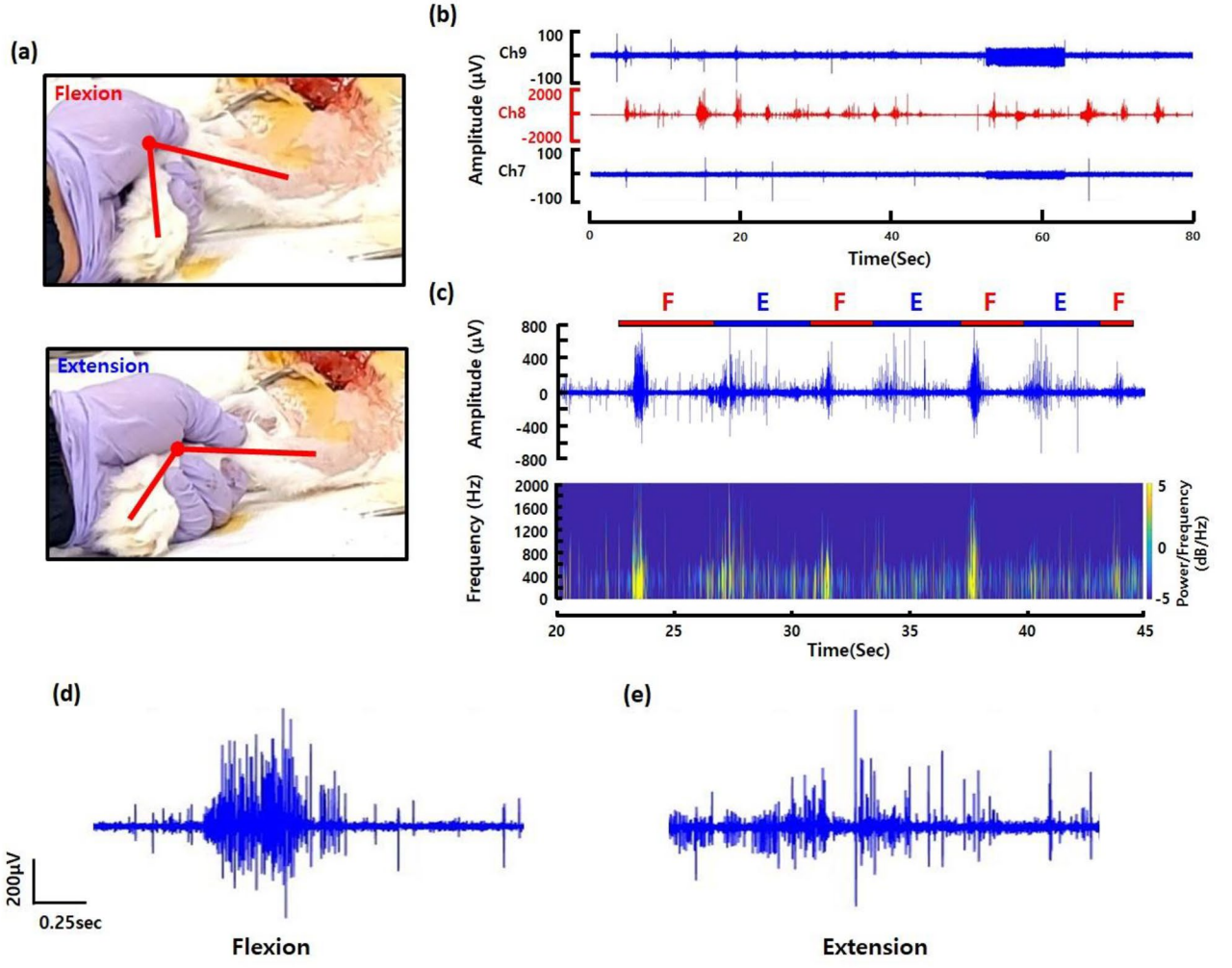

Fig. 4 Evoked sensory neural signals according to the movement of the ankle. (a) The angle of the ankle in flexion and extension states. (b) Neural signals in channels synchronized with ankle movement are represented in red color while nerve signals from channels that are not synchronized are represented in blue color. (c) Evoked sensory neural signals according to ankle movement in time and frequency domains (red bar: flexion state; blue bar: extension state). (d) The waveform of neural signal recorded in flexion state. (e) The waveform of neural signal recorded in extension state

nerve damage [19]. Therefore, it was assumed that the axons damaged by the FPMA insertion might be the source of the recorded burst-type spontaneous neural signals. On the other hand, channel 2 showed clear action potentials or spikes. A total of 4 spike units were detected by channel 2. Although the waveforms of the units were similar, the amplitude of each unit was different, so that clustering of spike units was possible through a commercial spike sorting program. The duration of the detected action potentials was about 4 ms. Also, the amplitudes of the spike units ranged from 130 μV up to 340 μV, with SNR of 3.1 up to 7.1 (Fig. 3c). Based on the recorded spike signals, it was confirmed that the implanted FPMA could effectively record spike signals from peripheral nerves.

Evoked sensory neural signal recording

After confirming the ability of the FPMA to record neural signals through spontaneous neural signal recording, we tried to record evoked neural signals generated by sensory stimulation. Various stimuli were applied to the FPMA-implanted leg. Among them, neural responses synchronized with ankle movement were detected (Fig. 4a).

In channel 8, multi-unit neural signals evoked by the ankle movement were recorded, while other channels did not show any related signal (Fig. 4b). It implies that the signals recorded by channel 8 were not artifacts caused by the ankle movement, but neural signals in response to the sensory stimulus of the ankle movement. Also, depending on the angle of the ankle, the neural signals showed different waveforms. Two types of waveforms appeared alternately according to the ankle position

(Fig. 4c). When the ankle flexed, the FPMA recorded compound neural signals. On the other hand, in the extension state, spikes of several units continuously fired (Fig. 4d and e). Especially, strong signals were generated when the ankle movement started. In addition, the frequency analysis showed that when the ankle was flexed, the strong signal was observed below 1000 Hz for a short duration of 500ms. On the other hand, in the extension state, it showed that the signal was weak over a longer period (Fig. 4c). It implies that the angle of the ankle could be specified based on the recorded nerve signals.

However, it is presumed that the evoked neural signals recorded in this study would not be neural signals originating from the proprioceptive axons. In previous studies, a characteristic of proprioceptive neural signals is that action potentials with a constant inter-spike interval continuously fires while a specific posture is maintained [20–22]. On the other hand, the neural signals recorded through the FPMA were multi-unit spikes, observed intensively when a particular posture started and then disappeared.

Based on these results, we concluded that the neural signals recorded by the FPMA were not from the axons responsible for muscle contraction, but axons involved in sensations associated with ankle movement. Although the recorded neural signals were not derived from proprioception, it still showed specific neural signal waveforms according to different angles of the ankle.

Conclusion

In this study, the FPMA successfully recorded neural signals from multiple axons in peripheral nerves. Action potentials from axons were successfully detected by 6 out of 9 channels of the FPMA used. In addition, we succeeded in recording evoked-sensory signals synchronized with the ankle movement. It shows that the FPMA can record sensory nerve signals from peripheral nerves with high resolution. In the future, we will chronically record sensory nerve signals to verify that the FPMA can be used in nerve-based prostheses to provide natural sensory feedback.

List of abbreviations

FPMA	Flexible penetrating microelectrode array
USEA	Utah slanted electrode array
PDMS	Polydimethylsiloxane
FPCB	Flexible printed circuit board
RIE	Reactive ion etching
PEG	Polyethylene glycol
BF	Biceps femoris muscle
RF	Rectus femoris muscle
TF	Tensor fasciae latae muscle
PCB	Printed circuit board
SNR	Signal-to-noise ratio
AP	Action potential

Acknowledgements

We acknowledge the Institute of Next-generation Semiconductor Convergence Technology and the Laboratory Animal Resource Center (LARC) at DGIST for all their kind support to conduct this study. In particular, we would like to thank Dr. Dong Jae Kim at LARC for his advice and help for animal experiments.

Authors' contributions

BWP designed and conducted animal experiments and performed data analysis. JWJ fabricated FPMAs and conducted animal experiments. BWP and JWJ wrote the manuscript. SK supervised the research and revised the manuscript. All authors read and approved the final manuscript.

Funding

This study was supported by the Basic Research Program (NRF-2020R1A2C2008833) through the National Research Foundation and the DGIST R&D Program (20-RT-01), funded by the Ministry of Science and ICT of Korea.

Availability of data and materials

The datasets used and/or analyzed during the current study are available from the corresponding author on reasonable request.

Declarations

Competing interests

The authors declare that they have no competing interests.

Received: 28 September 2022 / Accepted: 18 October 2022
Published online: 02 November 2022

References

1. Hermens H, Stramigioli S, Rietman H, Veltink P, Misra S (2011) Myoelectric forearm prostheses: State of the art from a user-centered perspective. J Rehabil Res Dev 48(6):719–773
2. Parajuli N, Sreenivasan N, Bifulco P, Cesarelli M, Savino S, Niola V, Esposito D, Hamilton TJ, Naik GR, Gunawardana U, Gargiulo GD (2019) Real-time EMG based pattern recognition control for hand prostheses: a review on existing methods, challenges and future implementation. Sensors 19(20):4596
3. Tavakoli M, Benussi C, Lourenco JL (2017) Single channel surface EMG control of advanced prosthetic hands: A simple, low cost and efficient approach. Expert Syst Appl 79:322–332
4. Yang D, Yang W, Huang Q, Liu H (2015) Classification of multiple finger motions during dynamic upper limb movements. IEEE J Biomed Health Inform 21(1):134–141
5. Tyler DJ (2015) Neural interfaces for somatosensory feedback: bringing life to a prosthesis. Curr Opin Neurol 28(6):574
6. Velliste M, Perel S, Spalding MC, Whitford AS, Schwartz AB (2008) Cortical control of a prosthetic arm for self-feeding. Nature 453(7198):1098–1101
7. Raspopovic S, Capogrosso M, Petrini FM, Bonizzato M, Rigosa J, Pino GD, Carpaneto J, Controzzi M, Boretius T, Fernandez E, Granata G, Oddo CM, Citi L, Ciancio AL, Cipriani C, Carrozza MC, Jensen W, Guglielmelli E, Stieglitz T, Rossini PM, Micera S (2014) Restoring natural sensory feedback in real-time bidirectional hand prostheses. Sci Transl Med 6(222):222ra19-222ra19.8
8. George JA, Kluger DT, Davis TS, Wendelken SM, Okorokova EV, He Q, Duncan CC, Hutchinson DT, Thumser ZC, Beckler DT, Marasco PD, Bensmaia SJ, Clark GA (2019) Biomimetic sensory feedback through peripheral nerve stimulation improves dexterous use of a bionic hand. Sci Robot 4(32):eaax2352
9. Vu PP, Vaskov AK, Irwin ZT, Henning PT, Lueders DR, Laidlaw AT, Davis AJ, Nu CS, Gates DH, Gillespie RB, Kemp SWP, Kung TA, Chestek CA, Cederna PS (2020) A regenerative peripheral nerve interface allows real-time control of an artificial hand in upper limb amputees. Sci Transl Med 12(533):eaay2857
10. Petrini FM, Bumbasirevic M, Valle G, Ilic V, Mijović P, Čvančara P, Barberi F, Katic N, Bortolotti D, Andreu D, Lechler K, Lesic A, Mazic S, Mijović B, Guiraud D, Stieglitz T, Alexandersson A, Micera S, Raspopovic S (2019) Sensory feedback restoration in leg amputees improves walking speed, metabolic cost and phantom pain. Nat Med 25(9):1356–1363

11. Raspopovic S, Cimolato A, Panarese A, Vallone F, Del Valle J, Micera S, Navarro X (2020) Neural signal recording and processing in somatic neuroprosthetic applications. A review. J Neurosci Methods 337:108653
12. Mastinu E, Engels LF, Clemente F, Dione M, Sassu P, Aszmann O, Brånemark R, Håkansson B, Controzzi M, Wessberg J, Cipriani C, Ortiz-Catalan M (2020) Neural feedback strategies to improve grasping coordination in neuromusculoskeletal prostheses. Sci Rep 10(1):1–14
13. George JA, Page DM, Davis TS, Duncan CC, Hutchinson DT, Rieth LW, Clark GA (2020) Long-term performance of Utah slanted electrode arrays and intramuscular electromyographic leads implanted chronically in human arm nerves and muscles. J Neural Eng 17(5):056042
14. Yan D, Jiman AA, Bottorff EC, Patel PR, Meli D, Welle EJ, Ratze DC, Havton LA, Chestek CA, Kemp SWP, Bruns TM, Yoon E, Seymour JP (2022) Ultraflexible and Stretchable Intrafascicular Peripheral Nerve Recording Device with Axon-Dimension, Cuff - Less Microneedle Electrode Array. Small 2200311
15. Christensen MB, Pearce SM, Ledbetter NM, Warren DJ, Clark GA, Tresco PA (2014) The foreign body response to the Utah Slant Electrode Array in the cat sciatic nerve. Acta Biomater 10(11):4650–4660
16. Byun D, Cho SJ, Lee BH, Min J, Lee JH, Kim S (2017) Recording nerve signals in canine sciatic nerves with a flexible penetrating microelectrode array. J Neural Eng 14(4):046023
17. Jang JW, Kang YN, Seo HW, Kim B, Choe HK, Park SH, Lee M, Kim S (2021) Long-term *in-vivo* recording performance of flexible penetrating microelectrode arrays. J Neural Eng 18(6):066018
18. Prasad A, Xue QS, Dieme R, Sankar V, Mayrand R, Nishida T, Streit W, Sanchez J (2014) Abiotic-biotic characterization of Pt/Ir microelectrode arrays in chronic implants. Front Neuroeng 7:2
19. Bernal L, Roza C (2018) Hyperpolarization-activated channels shape temporal patterns of ectopic spontaneous discharge in C - nociceptors after peripheral nerve injury. Eur J Pain 22(8):1377–1387
20. Crowe A, Matthews PBC (1964) The effects of stimulation of static and dynamic fusimotor fibres on the response to stretching of the primary endings of muscle spindles. J Physiol 174(1):109
21. Ackerley R, Samain-Aupic L, Ribot-Ciscar E (2022) Passive proprioceptive training alters the sensitivity of muscle spindles to imposed movements. Eneuro9(1)
22. Han S, Chu JU, Kim H, Park JW, Youn I (2017) Multiunit activity-based real-time limb-state estimation from dorsal root ganglion recordings. Sci Rep 7(1):1–14

Publisher's Note